Journal of Medical and Biological Engineering (2024) 44:499–513
https://doi.org/10.1007/s40846-024-00893-5

REVIEW ARTICLE

Artificial Intelligence as a Tool for Diagnosis of Cardiac Amyloidosis: A Systematic Review

Armia Ahmadi-Hadad[1] · Egle De Rosa[1] · Luigi Di Serafino[1] · Giovanni Esposito[1]

Received: 6 June 2024 / Accepted: 23 July 2024 / Published online: 6 August 2024

Abstract

Purpose Cardiac amyloidosis (CA) is a highly underdiagnosed disease characterized by the accumulation of misfolded amyloid protein fragments in the heart, resulting in reduced heart functionality and myocardial stiffness. Artificial intelligence (AI) has garnered considerable interest as a potential tool for diagnosing cardiovascular diseases, including CA. This systematic review concentrates on the application of AI in the diagnosis of CA.

Methods A comprehensive systematic search was performed on the databases of PubMed, Embase, and Medline, to identify relevant studies. The screening process was conducted in two stages, using predetermined inclusion and exclusion criteria, and was carried out in a blinded manner. In cases where discrepancies arose, the reviewers discussed and resolved the issue through consensus.

Results Following the screening process, a total of 10 studies were deemed eligible for inclusion in this review. These investigations evaluated the potential utility of AI models that analyzed routine laboratory data, medical records, ECG, transthoracic echocardiography, CMR, and WBS in the diagnosis of CA.

Conclusion AI models have demonstrated utility as a diagnostic tool for CA, with comparable or in one case superior efficacy to that of expert cardiologists.

Keywords Artificial intelligence · AI · Cardiac amyloidosis · Magnetic resonance · Imaging · ECG

Abbreviations

AI	Artificial intelligence
AL	Light chain amyloidosis
ATTR	Transthyretin amyloidosis
CA	Cardiac amyloidosis
CINE	Cardiac imaging with non-contrast enhancement
CMR	Cardiac magnetic resonance
CNN	Convolutional neural networks
CTS	Carpal tunnel syndrome
DL	Deep learning
DT	Decision tree
EF	Ejection fraction
GLS	Global longitudinal strain
HCM	Hypertrophic cardio myopathy
HF	Heart failure
LGE	Late gadolinium enhancement
LVEF	Left ventricular ejection fraction
LVH	Left ventricular hypertrophy
ML	Machine learning
PPV	Positive predictive value
RBF	Radial basis function
ROC AUC	Receiver operating characteristic area under the curve
SVM	Supervised machine learning
TTE	Transthoracic echocardiography
WBS	Whole-body scintigraphy

✉ Luigi Di Serafino
luigi.diserafino@unina.it

[1] Department of Advanced Biomedical Sciences, University of Naples Federico II, Naples, Italy

1 Introduction

Amyloidosis is a multisystemic pathological condition, in which incorrectly folded protein fragments accumulate in the extracellular compartment of various tissues [1–3]. Cardiac amyloidosis (CA) is linked to notable morbidity and mortality. The heightened utilization of cardiac magnetic resonance imaging (CMR) in the field of cardiology has uncovered an earlier unacknowledged prevalence of CA. Consequently, CA has transitioned from being a

"rare" ailment that was frequently diagnosed after death, to a condition of great clinical importance that every cardiologist must contend with [3, 4].

The misfolding of over 30 proteins can result in the development of amyloidosis [5]. Two types are particularly associated with the heart: the light chain-associated amyloid (AL) and transthyretin amyloid (ATTR). AL amyloidosis is associated with a disorder of clonal plasma cells of the bone marrow, while ATTR amyloidosis is caused by transthyretin misfolding [6, 7]. Transthyretin is a hepatically synthesized tetrameric protein that serves as a physiologic carrier for thyroxine and retinol [8]. ATTR could occur owing to deposition of wild-type transthyretin (ATTRwt), which is genetically normal, or it can be due to a mutant gene coding for transthyretin (ATTRv) [7, 9].

The therapeutical regimen for individuals recently diagnosed with AL amyloidosis involves a combination of dexamethasone, bortezomib, cyclophosphamide, and the monoclonal antibody daratumumab hyaluronidase (Dara-CyBorD). Furthermore, plasma cell (PC)-targeted treatments are frequently employed in clinical practice off-label [10]. In contrast, for ATTR, therapeutic approaches include the utilization of an RNA interference (RNAi) agent known as Patisiran, transthyretin tetramer stabilizers, such as tafamidis, and in instances of hereditary cases, liver transplantation are considered [11–13].

Without therapy, cardiac AL amyloidosis progresses rapidly and could be fatal [7, 14]. Conversely, the advancement of ATTR is more gradual. ATTRwt is associated with almost 3.5 years of survival, while the median survival is slightly less in ATTRv [7, 9, 15, 16].

Many possible applications for the use of AI in medicine are being explored. There are two main categories of AI. The first type is machine learning (ML), which is based on feature analysis, and the latter type is deep learning (DL), which can analyze imaging data, without the necessity of manual numerical data insertion [17, 18]. Machine learning, a scientific discipline integrating statistics and computational algorithms, consists of supervised and unsupervised learning. In medicine, supervised learning automates tasks like EKG interpretation, while unsupervised learning discovers intricate data patterns, especially in precision medicine for complex diseases [19]. Deep learning employs multi-layered neural networks to extract intricate patterns from data, achieving high accuracy in tasks like image recognition. It starts by identifying edges in various orientations and positions, progressively recognizing complex objects. This enables deep learning models to analyze images by discerning their distinct features and patterns [20]. Convolutional neural networks (CNNs) represent a class of sophisticated DL algorithms renowned for their exceptional proficiency in image analysis. These networks employ localized connections and parameter sharing, enabling the efficient extraction of distinctive features from images [20].

In this review, we will shed light on the use of ML, DL, and CNN in diagnosis of CA via different methods including ECG, MRI, TTE, and Bone Scintigraphy. In addition, we will compare the sensitivity and specificity of AI systems' diagnosis to expert physicians.

2 Materials and Methods

The protocol of this systematic review is registered in PROSPERO on 26/03/2023 with ID: CRD4202340847. This systematic review is accompanied by a PRISMA declaration (Fig. 1). The primary measure of interest in our investigation is the AI score, which reflects the level of diagnostic precision achieved by the AI system.

2.1 Search Strategy

Following an advanced search of Pubmed, Embase, and MEDLINE (OVID), databases on the 13 March 2023, we procured a sum of 47 papers, which were subsequently reduced to 23 after duplicate removal. Furthermore, two pertinent recent investigations have been incorporated into the publications yielded from the systematic search. The search was unconstrained by language or publication year. The supplementary material lists the search terms used in this study (Supplementary Appendix 1).

Two main reviewers (Armia Ahmadi-Hadad and Egle De Rosa) screened the papers in a blinded manner. In the first round, the titles and abstracts were subjected to screening, while in the second round, the full texts underwent scrutiny. Conflicting decisions were resolved by discussion. Ultimately, a pool of 10 papers was included in the meta-analysis (Fig. 1).

2.2 Inclusion and Exclusion Criteria

Studies investigating the use of AI in diagnosis of the CA were included. Our study criteria mandated the inclusion of studies written exclusively in English. This systematic review was not limited by any classification of amyloidosis subtype, as we incorporated relevant literature on ATTR and light chain amyloidosis without any exclusions. Publications were excluded if: (1) they did not mention AI; (2) CA was not the objective of the study; (3) the full text was not available.

2.3 Data Extraction and Synthesis

Text, tables, figures and supplementary materials were summarized in an Excel spreadsheet. Study design, type of

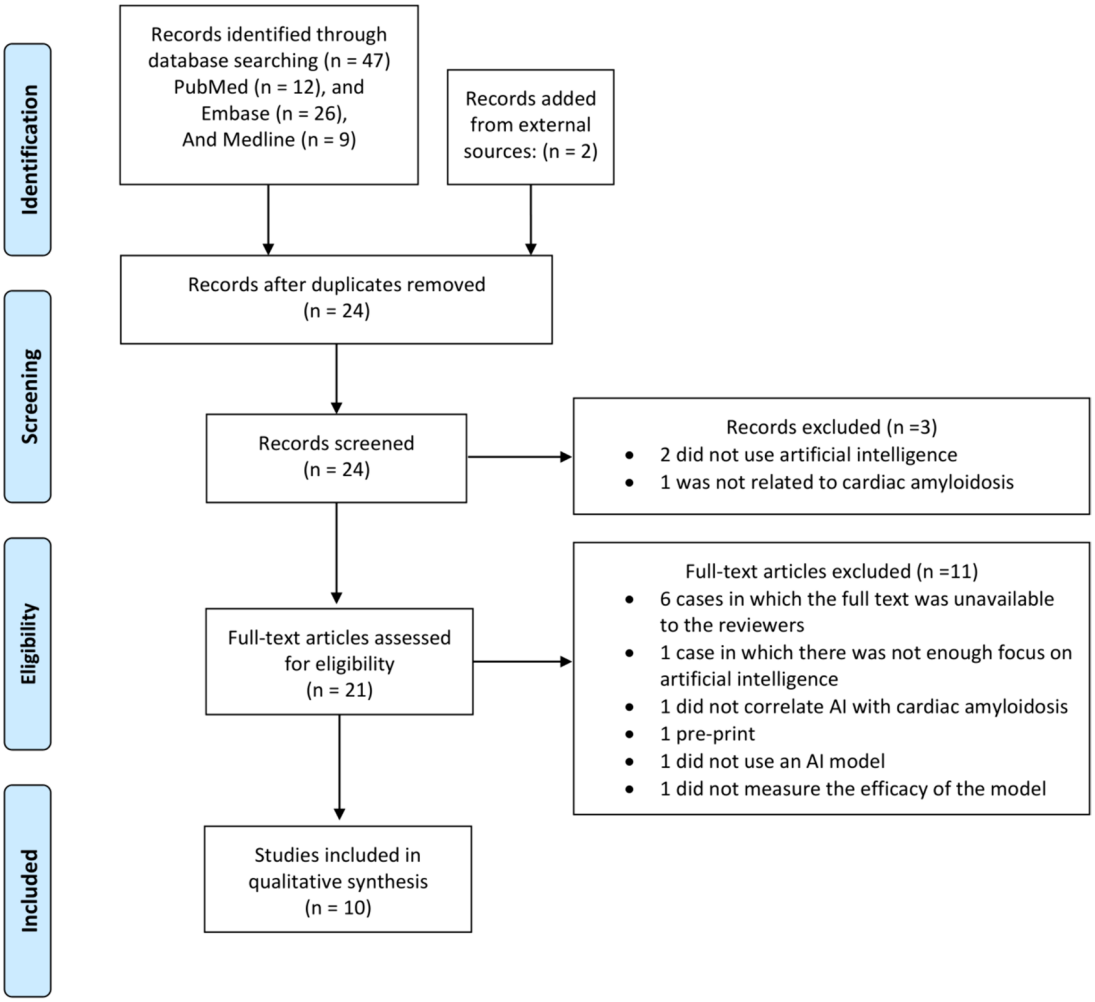

Fig. 1 PRISMA flow diagram. Preferred Reporting Items for Systematic Reviews and Meta-Analysis (PRISMA) flow diagram describing exclusions and inclusions. The preliminary search yielded a total of 47 results, following which duplicate outcomes were removed, and inclusion and exclusion criteria were applied in two rounds of screening. Ultimately, 10 studies were chosen to be included in the systematic review

control groups, number of patients involved in experimental and control groups, mean age of the patients, amyloidosis subtype, and type of the AI in use were extracted. Additionally, title, journal name, leading author, and publication year were collected.

2.4 Evaluation Metrics

Sensitivity, specificity, positive predictive value (PPV), ROC AUC, and F1-score were utilized in this systematic review. The receiver operating characteristic area under the curve (ROC AUC) score is a performance metric for binary classification models. It quantifies the ability of a model to distinguish between positive and negative cases by measuring the area under the ROC curve, where a higher AUC score indicates better discrimination. An AUC score of 1 signifies a perfect classifier, while 0.5 suggests random classification. The F1-score strikes a balance between precision, defined as the ratio of true positives to the sum of true positives and false positives, and recall, defined as the ratio of true positives to the sum of true positives and false negatives, by computing their harmonic mean. It was employed to evaluate the model's capability to minimize both false positives and false negatives, demonstrating its relevance to the research conducted in this paper.

3 Results

A systematic search of the PubMed, Embase and MEDLINE databases was conducted, yielding a total of 24 papers after duplicate removal. Out of the 24 abstracts screened, 3 abstracts were found to be ineligible. Subsequently, 21

full-text articles were evaluated for eligibility, with a total of 10 articles included in the systematic review (Fig. 1, Table 1).

The studies included in this review revealed that AI in different forms such as ML, DL, and CNN could be applied in different diagnostic tests, such as laboratory parameters [21], ECG [7, 22], CMR [3, 23, 24], TTE [22, 25, 26], Bone Scintigraphy [27], medical and nursing records [28] (Table 1).

The laboratory parameters model developed by Agibetov et al. achieved sensitivity, and specificity of 89.2% and 78.2% respectively with ROC AUC equal to 0.86 [21]. The medical and nursing records ML demonstrated sensitivity and specificity of 56% and 96% respectively with ROC AUC equal to 0.88 [28]. Among the TTE models, The ML introduced by Cotella et al. for identifying abnormal LVEF showed sensitivity and specificity of 83%, and 86% during the pre-CA TTE, and 70% and 79% at the time of CA diagnosis, respectively [25]. An TTE-based DL model developed by Duffy et al. demonstrated ROC AUC equal to 0.79 [26]. Moreover, an integrated ECG-TTE ML developed by Goto et al. showcased a 74–77% PPV [22]. Concerning the ECG models, the model developed by Grogan et al. demonstrated ROC AUC, and PPV equal to 0.91 and 0.86 respectively [7]. However, unlike the integrated ECG-TTE model of Goto et al. their sole-ECG model resulted in 3–4% PPV at 52–71% recall [22]. With regards to the CMR, the CNN model developed by Agibetov et al. exhibited a 0.96 ROC AUC [3]. However, the ML used by Eckstein et al. showed a ROC AUC equal to 0.962 and 0.996 for models using 10 and 41 variables respectively. The F1-score was reported 97% for the 41-variable group [23]. Martini et al. developed a DL and an ML model for CMR. The DL model showed an ROC AUC of 0.982 with sensitivity of 95% and a F1-score of 89%. The ML model showed comparable results to the DL ($p = 0.39$) with AUC equal to 0.952 [24].

Moreover, a WBS-based CNN model developed by Delbarre et al. demonstrated a sensitivity and specificity of 98.9% (± 1.0), and 99.5% (± 0.4) respectively and a ROC AUC of 0.999 for the fivefold cross validation group. For their external validation group sensitivity and specificity were 96.1% and 99.5% respectively with a corresponding ROC AUC of 0.999 [27].

4 Discussion

CA is a rare condition that is often underdiagnosed because its symptoms can resemble those of other cardiac pathologies [2, 29]. Moreover, CA frequently manifests in an insidious manner, rendering early-stage diagnosis challenging [30]. AI has the potential to be used as a screening tool to address this issue [28]. In this systematic review, we discuss various ML and DL tools that can analyse laboratory parameters, TTE, ECG, CMR, Bone Scintigraphy to take a significant step towards the development of a reliable and accurate automated diagnostic tool for CA.

4.1 Laboratory Parameters and Hospitalization Records

Agibetov et al. investigated the utilization of an expert-independent machine learning (ML) in differential diagnosis between patients with HF with or without AL/ATTR CA association through routine laboratory parameters. Hence, the prospect of discernible patterns in standard laboratory evaluations between CA-related HF as opposed to CA-unrelated HF was examined. Extensive knowledge regarding the types of HF that occur frequently is evident in the medical community. In contrast, uncommon HF subtypes such as those witnessed in CA are prone to eluding diagnosis or experiencing protracted delays during the diagnostic process. Rare diseases are frequently diagnosed in specialized medical centers, often at the conclusion of a protracted patient diagnostic process. In this study, 62 routine laboratory parameters, comprising clinical chemistry parameters, blood cell count, and coagulation parameters, were procured for algorithm development. Even though particular parameters, such as liver and kidney function parameters, were regularly established in every patient, others indicated a high degree of unavailability. In this investigation, an ML algorithm was adopted to enhance the accuracy of the baseline linear prediction model and to enable non-linear prediction, thereby improving the overall predictive performance. The model of logistic regression demonstrated a statistically significant correlation between lower risk factors of cardiovascular diseases, namely glucose ($p = 0.008$) and triglyceride ($p = 0.008$) levels in the bloodstream, and the presence of CA. The present finding implies that patients who develop HF due to CA may exhibit the condition in the absence of traditional cardiovascular risk factors, which are conventionally associated with ischemic heart disease and HFpEF [21].

Reduced concentrations of serum albumin and cholinesterase have been identified as potential indicators of compromised hepatic synthetic activity in patients with HF, particularly in cases of more advanced HF at the time of diagnosis in comparison to other HF subtypes. This observation may be attributed to delayed detection of CA in comparison to other HF subtypes [8]. The predictive models utilized by Agibetov et al. were all formulated using a training cohort of patients with CA ($n = 121$) and patients with HF but without CA ($n = 415$), as the foundation for their construction. A distinct prognostic validation cohort comprising 37 CA-positive and 124 CA-negative patients was employed to evaluate the performance of all prediction models. The optimal model, constructed by means of gradient-boosted ensembles of decision trees, outperforms the best linear model. Given

Table 1 List of included studies with number, age, and sex of the patients, AI algorithm types, study objectives, CA diagnosis methods, and outcomes

Study	Number of patients	Age	Male sex	AI Type	Study Objectives	CA diagnosis method	Outcome(s)
Agibetov et al. [21]	n = 124 for CA-unrelated HF; n = 36 for CA-related HF	CA-unrelated HF: 75.0 (69.0–78.0); CA-related HF: 78.0 (71.8–83.0)	CA-unrelated HF: 29.5%; CA-related HF: 77.8%	ML	The potential application of AI based on routine laboratory parameters for diagnosis of CA	Laboratory parameters	The top-performing model utilizing gradient-boosted decision tree ensembles attained an ROC AUC of 0.86, with sensitivity and specificity rates of 89.2% and 78.2%, respectively. In addition, the use of ML can produce a unique profile of HF related to CA that differs from HF unrelated to CA
Agibetov et al. [3]	n = 420 for CA-unrelated HF; n = 82 for CA-related HF	CA-unrelated HF: 66.0 (50.0–75.0); CA-related HF: 75.0 (68.0–82.5)	CA-unrelated HF: 44.9%; CA-related HF: 65.8%	CNN	The potential of CNN-based AI model for diagnosis of CA via analysing CMR	CMR	CNN performed a successful task in diagnosing the CA by analysing the CMR images. AI models achieved high diagnostic accuracy for patient classification, with the best-performing fine-tuned CNN achieving an average ROC AUC score of 0.96
García-García et al. [28]	2861 patients with HF; and 27 with CA	87 ± 17	42%	ML	ML as a means of diagnosing CA	Medical and nursing records gathered during hospital stays	This ML study demonstrated promising results for detecting CA in patients with HF and stroke, with a sensitivity of 0.56 and specificity of 0.96. The ML model exhibited excellent predictive performance, as evidenced by an area under the ROC curve of 0.88

Table 1 (continued)

Study	Number of patients	Age	Male sex	AI Type	Study Objectives	CA diagnosis method	Outcome(s)
Duffy et al. [26]	23,745 patients' Echo recordings were involved in this study (20,085 patients from Stanford Health Care (SHC) and 3660 from Cedars-Sinai Medical Center (CSMC))	Parasternal long-axis: from SHC: 61.6 ± 17.4, from CSMC: 62.8 ± 17.2; Apical 4-chamber: SHC: 69.1 ± 16.8, CSMC: 69.6 ± 14.7	Parasternal long-axis: from SHC: 45.8%, from CSMC: 38.3%; Apical 4-chamber: SHC: 46.0%, CSMC: 45.8%	DL	Using DL for detecting the increased left ventricular wall thickness, and finding its etiology, whether CA or hypertrophy	Echocardiography	The Echo recording-based DL algorithm demonstrated a noteworthy performance in the detection of CA and hypertrophic cardiomyopathy with AUC of 0.79 and 0.89 respectively
Eckstein et al. [23]	n = 44 for CTRL; n = 20 for HCM; n = 43 for CA	CTRL: 56.3 (52.5–62.9); HCM: 63.9 ± 7.4; CA: 79 (71–85)	CTRL: 52.27%; HCM: 50.00%; CA: 74.42%	ML	Potential utility of ML for detection of CA based on Right ventricular and bi-atrial strain and cardiac function	CMR	ML based on non-contrast CMR has the potential to support clinical decision-making for CA. Effectiveness of ML in detecting CA, with a detection rate of 82% (AUC 0.962) using the top 10 variables and 90.9% (AUC 0.996) using 41 variables. Specifically, the SVM RBF kernel exhibited a sensitivity of 100%, precision of 94%, and an F1-score of 97% in the 41-feature matrix utilized in this investigation
Cotella et al. [25]	n = 51 in total (AL-CA 11 (21.6%); ATTR + ATTR-wt 36 (70.6%); Undefined 4 (7.8%))	80.2 ± 9.7	52.94%	ML	Evaluation of potential use of AI for LVEF, and GLS calculation for in CA patients	Echocardiography	AI calculated GLS and LVEF are precise at both the pre-diagnosis and diagnosis phases. The sensitivity and specificity of the AI-generated indices for identifying abnormal LVEF was 83%, and 86% during the pre-CA echo, and 70% and 79% at the time of CA diagnosis, respectively

Table 1 (continued)

Study	Number of patients	Age	Male sex	AI Type	Study Objectives	CA diagnosis method	Outcome(s)
Delbarre et al. [27]	The external validation data comprised 1633 WBS images, encompassing 102 positive and 1531 negative cases	Sex and age below 90 years exerted a modest influence on performance	39.8% in the external validation data-set	CNN	Designing a CNN to identify substantial cardiac uptake (Perugini grade ≥ 2) on WBS sourced from extensive hospital databases	whole-body bone scintigraphy (WBS)	The constructed CNN demonstrated notable effectiveness in detecting CA For fivefold cross-validation: sensitivity: 98.9% (± 1.0), specificity: 99.5% (± 0.4), ROC AUC: 0.999 For external validation: sensitivity: 96.1%, specificity: 99.5%, ROC AUC: 0.999
Grogan et al. [7]	n = 508 for amyloidosis; n = 491 for control	68.1% over 60 years old for amyloidosis group; 67.6% over 60 years old for control group	Amyloidosis group: 73.6%; Control: 74.3%	Deep neural network	Potential application of AI in identifying CA from ECG	ECG	The AI tool was capable of predicting CA precisely. The AUC and PPV were 0.91 and 0.86 respectively for diagnosing either type of CA. In the studied population subgroup where serial ECGs were available, it was observed that the implementation of AI was able to identify the presence of CA in 60% of patients prior to clinical diagnosis

Table 1 (continued)

Study	Number of patients	Age	Male sex	AI Type	Study Objectives	CA diagnosis method	Outcome(s)
Martini et al. [24]	Patients with CA: n = 107; patients without CA: n = 99	For CA: 76 (69–81); for patients without CA: 73 (65–79)	CA: 74%; Patients without CA: 59%	ML, DL	Potential use of DL tools for diagnosing CA based on CMR	CMR	DL exhibited an admirable 88% diagnostic accuracy along with a remarkably high area under the curve (AUC) value of 0.982. Furthermore, the recall score (or sensitivity) achieved an impressive value of 95%, and both the F1 score and precision displayed notable scores with the F1 score at 89% and the precision at 83%. Additionally, an ML algorithm that scrutinized all CMR features manifested a diagnostic yield comparable to the DL strategy, as proven by an AUC value of 0.952 (p = 0.39)
Goto et al. [22]	CA patients in Echo group: n = 609 Control in Echo group: n = 3303 CA patients in ECG group: n = 597 Control in ECG group: n = 8612	For CA patients in Echo group (mean): 74.37 For control in Echo group (mean): 68.23 For CA patients in ECG group (mean): 70.28 For control in ECG group (mean): 63.22	CA patients in Echo group: 82.45% Control in Echo group: 67.37% CA patients in ECG group: 80.54% Control in ECG group: 64.14%	ML	The potential of AI in the precise identification of cardiac amyloidosis by means of echocardiography and ECG	ECG, Echocardiography	AI exhibits the potential to catalyse a transformative shift in the diagnosis of rare ailments such as CA, which pose a formidable challenge to conventional diagnostic approaches. The ECG ML model had 3 to 4% PPV at 52 to 71% recall. Pre-screening patients with ECG led to an improvement in the performance of the echocardiography model at 67% recall, with the PPV increasing from 33% to 74–77%

The data are reported as mean ± SD, median (range), or as a percentage

the specificity of both models, it is advisable to utilize these automated prediction methods primarily as a screening tool for identifying potential CA patients. Subsequently, supplementary confirmatory tests should be conducted to ensure accurate diagnoses. Moreover, given the rarity of CA as a form of HF, the aforementioned prediction models should not be used for general populations with a low disease prevalence (< 1%). Agibetov et al. implemented the algorithm on groups that displayed symptoms of HF, with a relatively high prevalence of amyloidosis at 23%, which is considered notable, considering that CA is a rare disease with a prevalence of 1 in 10,000 [21].

Similarly, an additional study conducted by García-García et al. has delved into the same technique of CA detection, further highlighting the abiding relevance of ML in the arena of CA diagnosis. In this investigation, information gathered from open-text medical and nursing records, acquired throughout hospitalization events served as the foundation for constructing an ML algorithm designed to diagnose cases of CA [28]. Given the chronic nature of the disease and the substantial number of elderly patients, effective healthcare cost management necessitates the exploration of efficient diagnostic methods. While structured clinical data informs, it incompletely elucidates disease progress. Conversely, unstructured information written by medical professionals may hold the key to understanding disease progression [28, 31]. This investigation involved the inclusion of both structured and unstructured records pertaining exclusively to subjects aged 65 years or above, as symptoms of ATTR typically manifest in this age group. To ensure a comprehensive analysis of potential patients, not restricted to those receiving cardiology or internal medicine care, the entire cohort of patients admitted to the hospital was considered for inclusion [28]. This approach could identify undiagnosed cases that might have been missed. The algorithmic prediction demonstrated superior outcomes when applied to the cohort of individuals afflicted with HF and CA disease. This method demonstrates a sensitivity of 0.56 and a high specificity of 0.96, ensuring minimal false positives [21, 28, 31]. However, its sensitivity of 0.56 indicates that it may not be suitable for a screening method, where high sensitivity is crucial for early detection. The diminished precision and modest F1 score can be rationalized by the low frequency of the ailment under investigation [32]. The detection of warning signals and significant terms discerned through algorithmic analysis has the potential to be employed in intelligent support systems embedded within electronic medical records. These systems can provide suggestions to clinicians when composing clinical evaluations by utilizing the identified keywords in the text. This application of technology can aid in decision-making and directly affect clinical care. Algorithms are incapable of establishing a cause-and-effect correlation and, as such, cannot replace the role of physicians in clinical practice. However, ML algorithms can recognize numerical patterns derived from vast amounts of healthcare data, which may not be readily apparent to humans [28]. The utilization of health care episodes for data treatment represents an innovative approach that enhances the identification of infrequent medical conditions. In this approach, the patient autonomously generates information that possesses adequate variability to be deemed distinct during the training of an ML algorithm. Enhancing the collection and interpretation of these multidimensional vectors can result in the revelation of novel trends that augment patient well-being or the effectiveness of the healthcare system [33].

4.2 Transthoracic Echography

A study conducted by Cotella et al. sought to evaluate the comparability between fully automated AI calculation of LVEF and global longitudinal strain (GLS) measurements with those obtained by conventional manual methods. The study was designed to evaluate the diagnostic efficacy of automated AI algorithms in detecting anomalies in individuals diagnosed with pre-clinical and clinical CA via TTE. The LVEF and GLS were measured from the apical 2- and 4-chamber views via both manual and automated approaches. Specifically, the EchoGo Core 2.0 software, developed by Ultromics, was employed in the automated measurements. The measurements of LVEF and GLS were subjected to dichotomization employing specific cutoff points. EF values below 50% and GLS values exceeding − 15.1% were utilized as the respective thresholds. The statistical analysis revealed that there were no statistically significant variations in the LVEF and GLS measurements obtained through manual and automated methods. This was observed both pre-clinical CA ($p = 0.791$ for LVEF and $p = 0.105$ for GLS, respectively) and at the time of diagnosis ($p = 0.463$ for LVEF and $p = 0.722$ for GLS, correspondingly). According to the results of the study, the sensitivity and specificity of AI-derived indices for detecting abnormal LVEF were found to be 83% and 86%, respectively, during the pre-CA TTE. However, these values decreased to 70% and 79%, respectively, at the time of CA diagnosis. Moreover, regarding the identification of abnormal GLS, in the pre-CA TTE, the AI-generated indices exhibited a sensitivity and specificity of 82% and 86%, respectively. Upon the diagnosis of CA, the sensitivity and specificity of the same indices were 100% and 67%, correspondingly. The etiology of the increased specificity observed in pre-CA compared to CA remains unclear; however, this discrepancy might result from image quality variations in the studies, limited sample size, unavailability of optimal apical-3-chamber (A3C) views for inclusion in left ventricular GLS analysis, and

the retrospective design of the study. However, considering the achieved successful results, extensive application of LVEF and GLS analysis via AI tools could potentially result in a more prompt evaluation of various disease states with accuracy and reproducibility that are comparable to manual methods [25]. Previous literature has reported that conventional echocardiographic parameters exhibit low diagnostic accuracy for CA, predominantly due to inadequate sensitivity [34]. However, patterns of myocardial deformation and global longitudinal strain have shown superior levels of sensitivity and specificity in diagnosis of CA [25]. Pagourelias et al. have demonstrated that the LVEF/GLS ratio is the optimal discriminating factor for CA, even in confronting challenging subsets within the patients [34]. Nonetheless, findings of Cotella et al. indicate that their LVEF/GLS ratio has poor sensitivity (25%) but good specificity (90%), which suggests that it could be potentially used as a rule-in diagnostic tool for CA. Moreover, by examining two distinct temporal points, it was demonstrated that utilization of the AI algorithms in these patients would enable the identification of CA aberrations even prior to the diagnosis, as stipulated by extant recommendations [25]. Furthermore, the utilization of AI in the calculation of GLS could present potential advantages in the follow up of CA patients. Cohen et al. [35] highlighted the critical role of GLS in evaluating CA. The authors reported that baseline GLS was an independent predictor of survival, surpassing conventional biomarkers. Moreover, a decrease in GLS by 2.0% at 12 and 24 month follow-up after clinical intervention correlated with improved long-term survival. These findings have significant clinical implications, particularly in the context of serial echocardiographic evaluations, which are typically performed on CA patients. Thus, the precise and reliable measurement of GLS is of paramount importance in the management of CA [25, 35].

In a multi-center investigation conducted by Goto et al. it was demonstrated that the echocardiographic model for the diagnosis of CA exhibits superior performance compared to the interpretation by expert cardiologists [22]. Novel TTE features have been identified, necessitating the acquisition of specialized software packages by healthcare providers. These packages are often time-consuming to operate and are consequently primarily utilized in clinical practice once a disease is suspected [22, 36]. However, an all-encompassing detection strategy, possessing genuine generalizability, ought not to necessitate any specialized acquisition or processing techniques, and it should exclusively rely on input data that is widely accessible to ensure its ubiquitous applicability. A video-based echocardiography model could serve as a potential solution to address this issue. In the model developed by Goto et al. a singular, widely-acquired view, known as the apical 4-chamber view (A4C), was employed, which can be obtained utilizing low-cost handheld ultrasound devices.

The detection of CA on TTE poses a significant challenge for human readers due to two primary issues. Firstly, there is a lack of adequately specific features within the echo videos. Secondly, there exists a requirement for specialized cardiologists to ensure the inclusion of a thorough examination of relevant features in every diagnostic study. However, integrating this task into existing clinical workflows can pose a challenge. The latter issue can be effectively resolved through the utilization of an AI system. Goto et al. aimed to assess the former issue through the execution of a direct comparison between two proficient human readers and an AI system regarding the diagnostic performance for CA using the test sets obtained from three distinct institutions. The findings of the study demonstrate that the automated system's AUC exhibited higher performance compared to that of human readers, across all cases examined, although in one case the outcome of the data analysis fell within the 95% confidence interval for one of the readers on one of the institute's data. (Predictive accuracy scores are illustrated in Table 1). Moreover, it is imperative to underscore the fact that the aforementioned model exhibited a discernibly superior performance in relation to ATTR amyloidosis as opposed to AL [22].

Duffy et al. used DL for measuring left ventricular wall thickness in order to detect possible cardiac hypertrophy, or cardiac amyloidosis. This endeavor holds significance owing to the inherent challenge in distinguishing etiological factors contributing to augmented ventricular wall thickness, encompassing hypertrophy, cardiomyopathy, and CA. This study encompassed a total of 23,745 patient records obtained from Stanford Health Care and Cedars-Sinai Medical Center. Echography video recordings from apical 4-chamber and parasternal long-axis views were employed for the study. Ultimately the external validation conducted within a domestic setting yielded an AUC equal to 0.79 and 0.89 respectively for the CA and hypertrophic cardiomyopathy [26].

4.3 ECG

AI models that employ ECG have the potential to function as a valuable tool for the timely diagnosis of CA due to their capacity to analyze multiple features in the ECG simultaneously. These features have been found to be linked with the early physiological alterations that occur during the disease. Furthermore, ECG alterations in conditions such as ischemia or left ventricular dysfunction may function as a premature indicator prior to the identification of structural changes through TTE, as well as preceding the onset of symptoms [8]. Electrocardiography of AL CA could be characterized by pseudoinfarct patterns

and low-voltage, which are present in 45% of cases. However, normal voltage does not exclude the diagnosis [37]. Moreover, in patients with ATTRwt, low voltage sign on ECG is present only in 25% of cases [9], moreover hypertrophy could be present in CA patients with ATTRwt [38], and ECG signs of LVH was observed in 20% of this type of patients. Abnormalities in ST-segment, T-wave, and conduction system are commonly present in both types of CA; however, they are not CA specific [7]. A research investigation carried out by Grogan et al. [7] examined the utility of a deep neural network, trained on ECG data as a diagnostic tool to detect CA at the Mayo Clinic. The study comprised a sample size of 4995 patients, including both cases and controls. The experimental evaluations were conducted utilizing the 6-lead and single-lead ECG modalities. The AUC exhibited a value of 0.91, alongside a PPV of 0.86 for the purpose of diagnosing either type of CA. Additionally, the AI algorithm was able to accurately predict the presence of CA in 59% of cases included in the pre-diagnostic electrocardiogram study, at least 6 months prior to the clinical diagnosis. The top performing single-lead algorithm was V5, which was associated with AUC and precision of 0.86 and 0.78 respectively. Other single lead algorithms demonstrated approximately the same performance. However, the 6-lead model proved to be more effective with AUC and precision of 0.90 and 0.85 correspondingly. By enabling adaptation for both single-lead and 6-lead ECG measurements, screening for CA would become possible using smartphone-enabled electrodes. Grogan et al. suggest that the deep neural network developed can detect physiologic ECG changes, which are specific to CA and are not recognized by conventional ECG analysis. Conferring additional advantages in the context of CA, the AI-ECG model may hold the potential to propose the diagnosis of ATTRwt amyloidosis in females. Despite the commonly reported male preponderance of over 90% in most studies to date, female patients are susceptible to the development of ATTRwt amyloidosis and may be subject to underdiagnosis. In such cases where classic echocardiographic characteristics are absent, the AI-ECG model may have the potential to propose the diagnosis of ATTRwt amyloidosis in females [7].

Similarly, Goto et al. utilized an ECG based ML algorithm. Additionally, they developed an integrated ECG-TTE model to enhance the diagnostic performance. The PPV of the ECG-based AI model was found to be in the range of 3–4% at a recall of 52–71%. The results indicate that pre-screening with ECG significantly enhanced the TTE model's performance at a recall of 67%, resulting in an improved PPV of 74–77% compared to a PPV of 33% without pre-screening [22].

4.4 CMR

CMR is also recognized as a diagnostic tool for detecting and characterizing CA. However, in specific scenarios, CMR imaging may not be sufficient to establish a dependable diagnosis of CA. Currently, the most informative diagnostic assessment for TTR CA is represented by DPD bone scintigraphy. Conversely, DPD bone scintigraphy may frequently yield normal results and lack reliability in detecting AL CA. Furthermore, despite the potential lack of specificity in the manifestations of AL CA on CMR scans, and the occasional occurrence of a normal CMR in the presence of AL CA, CMR remains a valuable diagnostic modality for AL CA, as underlying pathological status, such as plasma cell dyscrasia, can be detected with the aid of CMR imaging [3, 39, 40].

In MRI centers with low referral volumes, there exists a risk of neglecting the detection of CA during the interpretation process [3]. Agibetov et al. [3] employed a DL model (specifically CNN) to devise a completely automated algorithm for the diagnosis of CA via CMR. Different protocols were used for developing the AI model including late gadolinium enhancement (LGE), Modified look-locker inversion recovery (MOLLI), and Cardiac Imaging with non-contrast enhancement (CINE). Specifically, the algorithms trained using LGE, outperformed the other models in the study [3]. LGE enables the identification of distinctive patterns, such as the expedited elimination of gadolinium from the myocardium and blood pool, in comparison to nonamyloid control individuals [41]. The CNN model, which exhibited the highest level of performance in this study, attained an average ROC AUC score of 0.96, thereby yielding a diagnostic accuracy of 90% specificity and 94% sensitivity. By comparing the performance of AI models across various data modalities, it has been observed that the models that are capable of processing CMR images demonstrate the highest level of diagnostic accuracy in general. Agibetov et al. demonstrated that AI prediction models may not necessitate any advanced understanding of CA and could be independent of a particular imaging protocol [3]. Agibetov et al. were unable to utilize AI to differentiate between AL and ATTR amyloidosis due to the scarcity of CA and consequently, the limited number of available samples [3]. However, transmural and subendocardial LGE patterns exhibit distinguishing features that could differentiate AL from ATTR [40]. These findings imply a promising prospect for the application of AI in differentiating between these two subtypes. Another study carried out by Eckstein et al. [23] used a SVM algorithm based on cardiac function (EF in specific) and multi-chamber strain including strain measurements of the left and right atria and right ventricle for diagnosis of CA. Various types of AI algorithms were employed in this study, including K-Nearest Neighbor (KNN), Supervised machine learning (SVM) linear, SVM radial basis function (RBF) kernel,

Table 2 Risk of bias assessment with QUADAS

Study	Risk of bias				Applicability concerns		
	Patient selection	Index test	Reference standard	Flow and timing	Patient selection	Index test	Reference standard
Agibetov et al. [21]	—	?	–	?	–	–	–
Agibetov et al. [3]	–	?	–	—	–	–	–
García-García et al. [28]	?	?	?	?	–	–	?
Duffy et al. [26]	–	–	–	?	–	–	–
Jan Eckstein et al. [23]	–	–	–	?	–	–	–
Cotella et al. [25]	?	–	–	—	–	–	–
Delbarre et al. [27]	–	–	–	–	–	–	–
Grogan et al. [7]	—	—	?	—	–	–	–
Martini et al. [24]	–	?	–	?	–	–	–
Goto et al. [22]	—	–	–	—	–	–	–

– low risk, — high risk, ? unclear risk

and decision tree (DT). The application of SVM algorithms has demonstrated high accuracy in distinguishing CA from a cohort of HCM patients and control subjects. The aforementioned study presents novel insights into the use of non-contrast CMR imaging for diagnostic purposes, with the potential to aid clinical decision-making. Results indicate that a SVM RBF kernel outperforms other algorithms, achieving high diagnostic accuracy under supervision. SVM RBF kernel demonstrated a diagnostic accuracy of 90.9%, AUC of 0.996, Sensitivity of 100%, Precision of 94%, and F1-Score of 97% in the 41-feature matrix employed in this study.

Martini et al. [24] conducted a comparative analysis of DL and ML algorithms considering all features collected through manual methods (left ventricular volume, distribution of LGE, early darkening of the blood-pool, function, mass, pleural and pericardial effusion, etc.), to compare the accuracy of the DL model to an ML human reading stimulation model. In this study the assessment of LGE CMR obtained from the short axis, as well as 2 and 4-chamber views was performed by three DL networks. The results of the comparison between the ML and DL models indicated that the DL approach showed a comparable diagnostic performance to the ML-based approach for the detection of CA (Table 1).

4.5 Bone Scintigraphy

Delbarre et al. designed a convolutional neural network model aiming at automatic identification of significant cardiac uptake on technetium-99 m, defined as Perugini grade equal to or greater than 2, on whole-body scintigraphy (WBS) images sourced from extensive hospital databases. This model extremely facilitates the identification of patients at risk of CA. This study used two validation methods. Fivefold cross-validation involves dividing a dataset into five equal subsets. Subsequently, the model is trained on four of these subsets while the fifth is used for testing. External validation, on the other hand, refers to testing a model on a separate dataset (in this case an independent hospital) that was not used during the model's training or validation process. The fivefold cross-validation yielded 98.9% (± 1.0) sensitivity, 99.5% (± 0.4) specificity, and a ROC AUC equal to 0.999 (SD = 0.000), while external validation yielded 96.1% sensitivity, 99.5% specificity, and a ROC AUC equal to 0.999. In light of these favorable outcomes and the substantial frequency at which WBS is performed worldwide, this approach possesses the capacity to function as a screening modality for TTR-CA [27].

5 Risk of Bias Assessment

Risk of bias was evaluated by the Quality Assessment of Diagnostic Accuracy Studies (QUADAS-2) [42]. Table 2 summarizes the risk of bias assessment outcomes.

6 Conclusions

The implementation of AI algorithms in both forms of ML and DL provides an efficient method for analyzing multiple diagnostic modalities, including laboratory parameters, hospitalization records, TTE, ECG, and Bone Scintigraphy. ML models based on routine laboratory parameters and open-text medical and nursing records have demonstrated utility in the detection of CA. Similarly, an ML model using LVEF and GLS measurements obtained from TTE has demonstrated high efficacy in the identification of both pre-clinical and clinical CA. The TTE model was

reported in one instance to have better diagnostic performance compared with expert cardiologists. ECG-based models were able to identify pre-clinical CA through recognition of physiological ECG patterns. In addition, AI models using LGE sequences have showed high effectiveness in the diagnosis of CA. Overall, the integration of AI tools presents a promising avenue for advancing the diagnosis of CA even further.

Finally, we might suggest a three-step approach for CA diagnosis using AI tools:

1. Asymptomatic individuals could be screened for CA using ECG AI models.
2. Patients with suspected CA could be screened further using AI-models including ECG and TTE data.
3. Symptomatic patients may benefit from AI models including routine laboratory data, MRI, and Bone Scintigraphy.

Supplementary Appendix 1

PubMed:

("AI"[tw] OR "Artificial intelligence"[tw]) AND ("cardiac amyloidosis"[tw]) NOT ("Apolipoprotein*"[tw] OR "APO*"[tw])

Embase:

('AI':ti OR 'Artificial intelligence':ti) AND ('cardiac amyloidosis':ti) NOT ('Apolipoprotein*':ti,ab,kw,de OR 'APO*':ti,ab,kw,de)

Medline:

("AI".tw. OR "Artificial intelligence".tw.) AND ("cardiac amyloidosis".tw.) NOT ("Apolipoprotein*".tw. OR "APO*".tw.)

Author Contributions Armia Ahmadi-Hadad, Egle De Rosa, Luigi Di Serafino, and Giovanni Esposito have participated in the conception and design of the study, data acquisition, drafting the article, critical revision, and final approval of the submitted version. In addition to having the aforementioned roles Armia Ahmadi-Hadad and Egle De Rosa contributed to the systematic review rounds.

Funding Open access funding provided by Università degli Studi di Napoli Federico II within the CRUI-CARE Agreement. None.

Data availability Not applicable.

Declarations

Conflict of interest Dr. Di Serafino reports personal fees from Abbott Vascular and Hexacath, outside the submitted work. Prof. Esposito reports personal fees from Abbott Vascular, Amgen, Boehringer Ingelheim, Edwards Lifesciences, Terumo, and Sanofi, outside the submitted work and research grants to the institution from Alvimedica, Boston Scientific, and Medtronic. Armia Ahmadi-Hadad and Egle De Rosa have no conflicts of interest to declare.

References

1. Palladini, G., Campana, C., Klersy, C., Balduini, A., Vadacca, G., Perfetti, V., Perlini, S., Obici, L., Ascari, E., d'Eril, G. M., & Moratti, R. (2003). Serum N-terminal Pro-brain natriuretic peptide is a sensitive marker of myocardial dysfunction in AL amyloidosis. *Circulation, 107*(19), 2440–2445. https://doi.org/10.1161/01.CIR.0000068314.02595.B2
2. Falk, R. H., Alexander, K. M., Liao, R., & Dorbala, S. (2016). AL (light-chain) cardiac amyloidosis. *Journal of the American College of Cardiology, 68*(12), 1323–1341. https://doi.org/10.1016/j.jacc.2016.06.053
3. Agibetov, A., Kammerlander, A., Duca, F., Nitsche, C., Koschutnik, M., Donà, C., Dachs, T. M., Rettl, R., Stria, A., Schrutka, L., & Binder, C. (2021). Convolutional neural networks for fully automated diagnosis of cardiac amyloidosis by cardiac magnetic resonance imaging. *Journal of Personalized Medicine, 11*(12), 1268. https://doi.org/10.3390/jpm11121268
4. Tanskanen, M., Peuralinna, T., Polvikoski, T., Notkola, I. L., Sulkava, R., Hardy, J., Singleton, A., Kiuru-Enari, S., Paetau, A., Tienari, P. J., & Myllykangas, L. (2008). Senile systemic amyloidosis affects 25% of the very aged and associates with genetic variation in alpha2-macroglobulin and tau: A population-based autopsy study. *Annals of Medicine, 40*(3), 232–239. https://doi.org/10.1080/07853890701842988
5. Garcia-Pavia, P., Rapezzi, C., Adler, Y., Arad, M., Basso, C., Brucato, A., Burazor, I., Caforio, A. L., Damy, T., Eriksson, U., & Fontana, M. (2021). Diagnosis and treatment of cardiac amyloidosis: A position statement of the ESC working group on myocardial and pericardial diseases. *European Heart Journal, 42*(16), 1554–1568. https://doi.org/10.1093/eurheartj/ehab072
6. Gertz, M. A., Dispenzieri, A., & Sher, T. (2015). Pathophysiology and treatment of cardiac amyloidosis. *Nature Reviews Cardiology, 12*(2), 91–102. https://doi.org/10.1038/nrcardio.2014.165
7. Grogan, M., Lopez-Jimenez, F., Cohen-Shelly, M., Dispenzieri, A., Attia, Z. I., Abou Ezzedine, O. F., Lin, G., Kapa, S., Borgeson, D. D., Friedman, P. A., & Murphree, D. H., Jr. (2021). Artificial intelligence-enhanced electrocardiogram for the early detection of cardiac amyloidosis. *Mayo Clinic Proceedings, 96*(11), 2768–2778. https://doi.org/10.1016/j.mayocp.2021.04.023
8. Martinez-Naharro, A., Hawkins, P. N., & Fontana, M. (2018). Cardiac amyloidosis. *Clinical Medicine, 18*(2), s30–s35. https://doi.org/10.7861/clinmedicine.18-2-s30
9. Ruberg, F. L., Grogan, M., Hanna, M., Kelly, J. W., & Maurer, M. S. (2019). Transthyretin amyloid cardiomyopathy. *Journal of the American College of Cardiology, 73*(22), 2872–2891. https://doi.org/10.1016/j.jacc.2019.04.003
10. Bianchi, G., Zhang, Y., & Comenzo, R. L. (2021). AL amyloidosis: Current chemotherapy and immune therapy treatment strategies. *JACC CardioOncology, 3*(4), 467–487. https://doi.org/10.1016/j.jaccao.2021.09.003

11. Ando, Y., Coelho, T., Berk, J. L., Cruz, M. W., Ericzon, B. G., Ikeda, S. I., Lewis, W. D., Obici, L., Planté-Bordeneuve, V., Rapezzi, C., & Said, G. (2013). Guideline of transthyretin-related hereditary amyloidosis for clinicians. *Orphanet Journal of Rare Diseases, 8*(1), 31. https://doi.org/10.1186/1750-1172-8-31
12. Castaño, A., Drachman, B. M., Judge, D., & Maurer, M. S. (2015). Natural history and therapy of TTR-cardiac amyloidosis: Emerging disease-modifying therapies from organ transplantation to stabilizer and silencer drugs. *Heart Failure Reviews, 20*(2), 163–178. https://doi.org/10.1007/s10741-014-9462-7
13. Adams, D., Gonzalez-Duarte, A., O'Riordan, W. D., Yang, C. C., Ueda, M., Kristen, A. V., Tournev, I., Schmidt, H. H., Coelho, T., Berk, J. L., & Lin, K. P. (2018). Patisiran, an RNAi therapeutic, for hereditary transthyretin amyloidosis. *New England Journal of Medicine, 379*(1), 11–21. https://doi.org/10.1056/NEJMoa1716153
14. Muchtar, E., Gertz, M. A., Kumar, S. K., Lacy, M. Q., Dingli, D., Buadi, F. K., Grogan, M., Hayman, S. R., Kapoor, P., Leung, N., & Fonder, A. (2017). Improved outcomes for newly diagnosed AL amyloidosis between 2000 and 2014: Cracking the glass ceiling of early death. *Blood, 129*(15), 2111–2119. https://doi.org/10.1182/blood-2016-11-751628
15. Grogan, M., Scott, C. G., Kyle, R. A., Zeldenrust, S. R., Gertz, M. A., Lin, G., Klarich, K. W., Miller, W. L., Maleszewski, J. J., & Dispenzieri, A. (2016). Natural history of wild-type transthyretin cardiac amyloidosis and risk stratification using a novel staging system. *Journal of the American College of Cardiology, 68*(10), 1014–1020. https://doi.org/10.1016/j.jacc.2016.06.033
16. Gillmore, J. D., Maurer, M. S., Falk, R. H., Merlini, G., Damy, T., Dispenzieri, A., Wechalekar, A. D., Berk, J. L., Quarta, C. C., Grogan, M., & Lachmann, H. J. (2016). Nonbiopsy diagnosis of cardiac transthyretin amyloidosis. *Circulation, 133*(24), 2404–2412. https://doi.org/10.1161/CIRCULATIONAHA.116.021612
17. Slomka, P. J., Miller, R. J., Isgum, I., & Dey, D. (2020). Application and translation of artificial intelligence to cardiovascular imaging in nuclear medicine and noncontrast CT. *Seminars in Nuclear Medicine, 50*(4), 357–366. https://doi.org/10.1053/j.semnuclmed.2020.03.004
18. Slomka, P. J., Moody, J. B., Miller, R. J. H., Renaud, J. M., Ficaro, E. P., & Garcia, E. V. (2021). Quantitative clinical nuclear cardiology, part 2: Evolving/emerging applications. *Journal of Nuclear Cardiology, 28*(1), 115–127. https://doi.org/10.1007/s12350-020-02337-4
19. Deo, R. C. (2015). Machine learning in medicine. *Circulation, 132*(20), 1920–1930. https://doi.org/10.1161/CIRCULATIONAHA.115.001593
20. LeCun, Y., Bengio, Y., & Hinton, G. (2015). Deep learning. *Nature, 521*(7553), 436–444. https://doi.org/10.1038/nature14539
21. Agibetov, A., Seirer, B., Dachs, T. M., Koschutnik, M., Dalos, D., Rettl, R., Duca, F., Schrutka, L., Agis, H., Kain, R., & Auer-Grumbach, M. (2020). Machine learning enables prediction of cardiac amyloidosis by routine laboratory parameters: A proof-of-concept study. *Journal of Clinical Medicine, 9*(5), 1334. https://doi.org/10.3390/jcm9051334
22. Goto, S., Mahara, K., Beussink-Nelson, L., Ikura, H., Katsumata, Y., Endo, J., Gaggin, H. K., Shah, S. J., Itabashi, Y., MacRae, C. A., & Deo, R. C. (2021). Artificial intelligence-enabled fully automated detection of cardiac amyloidosis using electrocardiograms and echocardiograms. *Nature Communications, 12*(1), 2726. https://doi.org/10.1038/s41467-021-22877-8
23. Eckstein, J., Moghadasi, N., Körperich, H., Weise Valdés, E., Sciacca, V., Paluszkiewicz, L., Burchert, W., & Piran, M. (2022). A machine learning challenge: Detection of cardiac amyloidosis based on Bi-atrial and right ventricular strain and cardiac function. *Diagnostics, 12*(11), 2693. https://doi.org/10.3390/diagnostics12112693
24. Martini, N., Aimo, A., Barison, A., Della Latta, D., Vergaro, G., Aquaro, G. D., Ripoli, A., Emdin, M., & Chiappino, D. (2020). Deep learning to diagnose cardiac amyloidosis from cardiovascular magnetic resonance. *Journal of Cardiovascular Magnetic Resonance, 22*(1), 84. https://doi.org/10.1186/s12968-020-00690-4
25. Cotella, J. I., Slivnick, J. A., Sanderson, E., Singulane, C., O'Driscoll, J., Asch, F. M., Addetia, K., Woodward, G., & Lang, R. M. (2023). Artificial intelligence based left ventricular ejection fraction and global longitudinal strain in cardiac amyloidosis. *Echocardiography, 40*(3), 188–195. https://doi.org/10.1111/echo.15516
26. Duffy, G., Cheng, P. P., Yuan, N., He, B., Kwan, A. C., Shun-Shin, M. J., Alexander, K. M., Ebinger, J., Lungren, M. P., Rader, F., & Liang, D. H. (2022). High-throughput precision phenotyping of left ventricular hypertrophy with cardiovascular deep learning. *JAMA Cardiology, 7*(4), 386. https://doi.org/10.1001/jamacardio.2021.6059
27. Delbarre, M. A., Girardon, F., Roquette, L., Blanc-Durand, P., Hubaut, M. A., Hachulla, É., Semah, F., Huglo, D., Garcelon, N., Marchal, E., & El Esper, I. (2023). Deep learning on bone scintigraphy to detect abnormal cardiac uptake at risk of cardiac amyloidosis. *JACC Cardiovascular Imaging, 16*(8), 1085–1095. https://doi.org/10.1016/j.jcmg.2023.01.014
28. García-García, E., González-Romero, G. M., Martín-Pérez, E. M., Zapata Cornejo, E. D. D., Escobar-Aguilar, G., & Cárdenas Bonnet, M. F. (2021). Real-world data and machine learning to predict cardiac amyloidosis. *International Journal of Environmental Research and Public Health, 18*(3), 908. https://doi.org/10.3390/ijerph18030908
29. Ponikowski, P., Voors, A. A., Anker, S. D., Bueno, H., Cleland, J. G., Coats, A. J., Falk, V., González-Juanatey, J. R., Harjola, V. P., Jankowska, E. A., & Jessup, M. (2016). 2016 ESC guidelines for the diagnosis and treatment of acute and chronic heart failure. *European Heart Journal, 37*(27), 2129–2200. https://doi.org/10.1093/eurheartj/ehw128
30. Lane, T., Fontana, M., Martinez-Naharro, A., Quarta, C. C., Whelan, C. J., Petrie, A., Rowczenio, D. M., Gilbertson, J. A., Hutt, D. F., Rezk, T., & Strehina, S. G. (2019). Natural history, quality of life, and outcome in cardiac transthyretin amyloidosis. *Circulation, 140*(1), 16–26. https://doi.org/10.1161/CIRCULATIONAHA.118.038169
31. Basharat, I., Raza, A., Fatima, M., Qamar, U., & Ahmed, S. (2016). A framework for classifying unstructured data of cardiac patients: A supervised learning approach. *International Journal of Advanced Computer Science and Applications*. https://doi.org/10.14569/IJACSA.2016.070218
32. Garg, R., Dong, S., Shah, S., & Jonnalagadda, S. R. (2016). A bootstrap machine learning approach to identify rare disease patients from electronic health records. Preprint retrieved from https://arxiv.org/abs/1609.01586
33. Sheikhalishahi, S., Miotto, R., Dudley, J. T., Lavelli, A., Rinaldi, F., & Osmani, V. (2019). Natural language processing of clinical notes on chronic diseases: Systematic review. *JMIR Medical Informatics, 7*(2), e12239. https://doi.org/10.2196/12239
34. Pagourelias, E. D., Mirea, O., Duchenne, J., Van Cleemput, J., Delforge, M., Bogaert, J., Kuznetsova, T., & Voigt, J. U. (2017). Echo parameters for differential diagnosis in cardiac amyloidosis. *Circulation: Cardiovascular Imaging*. https://doi.org/10.1161/CIRCIMAGING.116.005588
35. Cohen, O. C., Ismael, A., Pawarova, B., Manwani, R., Ravichandran, S., Law, S., Foard, D., Petrie, A., Ward, S., Douglas, B., & Martinez-Naharro, A. (2022). Longitudinal strain is an independent predictor of survival and response to therapy in patients with systemic AL amyloidosis. *European Heart Journal, 43*(4), 333–341. https://doi.org/10.1093/eurheartj/ehab507

36. Phelan, D., Collier, P., Thavendiranathan, P., Popović, Z. B., Hanna, M., Plana, J. C., Marwick, T. H., & Thomas, J. D. (2012). Relative apical sparing of longitudinal strain using two-dimensional speckle-tracking echocardiography is both sensitive and specific for the diagnosis of cardiac amyloidosis. *Heart, 98*(19), 1442–1448. https://doi.org/10.1136/heartjnl-2012-302353
37. Murtagh, B., Hammill, S. C., Gertz, M. A., Kyle, R. A., Tajik, A. J., & Grogan, M. (2005). Electrocardiographic findings in primary systemic amyloidosis and biopsy-proven cardiac involvement. *The American Journal of Cardiology, 95*(4), 535–537. https://doi.org/10.1016/j.amjcard.2004.10.028
38. Maleszewski, J. J. (2015). Cardiac amyloidosis: Pathology, nomenclature, and typing. *Cardiovascular Pathology, 24*(6), 343–350. https://doi.org/10.1016/j.carpath.2015.07.008
39. Bonderman, D., Agis, H., Kain, R., & Mascherbauer, J. (2016). Amyloid in the heart: An under-recognized threat at the interface of cardiology, haematology, and pathology. *European Heart Journal Cardiovascular Imaging, 17*(9), 978–980. https://doi.org/10.1093/ehjci/jew130
40. Bonderman, D., Pölzl, G., Ablasser, K., Agis, H., Aschauer, S., Auer-Grumbach, M., Binder, C., Dörler, J., Duca, F., Ebner, C., & Hacker, M. (2020). Diagnosis and treatment of cardiac amyloidosis: An interdisciplinary consensus statement. *Wiener klinische Wochenschrift, 132*(23–24), 742–761. https://doi.org/10.1007/s00508-020-01781-z
41. Maceira, A. M., Joshi, J., Prasad, S. K., Moon, J. C., Perugini, E., Harding, I., Sheppard, M. N., Poole-Wilson, P. A., Hawkins, P. N., & Pennell, D. J. (2005). Cardiovascular magnetic resonance in cardiac amyloidosis. *Circulation, 111*(2), 186–193. https://doi.org/10.1161/01.CIR.0000152819.97857.9D
42. Whiting, P. F. (2011). QUADAS-2: A revised tool for the quality assessment of diagnostic accuracy studies. *Annals of Internal Medicine, 155*(8), 529. https://doi.org/10.7326/0003-4819-155-8-201110180-00009